Ships and Offshore Structures, 2014
Vol. 9, No. 3, 266–271, http://dx.doi.org/10.1080/17445302.2013.792457

Dynamic snap-through of a negative shallow arch resting on a fluid layer

Ahmed Anwar*, Mohamed Taha and Mohamed Nassar

Mathematics and Physics Engineering Department, Faculty of Engineering, Cairo University, Giza, Egypt

(*Received 16 October 2012; final version received 2 April 2013*)

In this paper, we study the snap-through stability of a negative shallow arch resting on a fluid layer foundation under a point load moving at a constant speed. The deformation of the arch is expressed in the Fourier series. By studying the fluid layer separately, it is noted that the back pressure of the fluid is directly proportional to the density of the fluid and depth of the fluid layer. We are interested only when the point load is downward. In quasi-static manner, it is so obvious that the arch will not snap. When the point load moves with a significant speed, we used the first four modes in the Fourier series to predict the response of the arch.

Keywords: snap-through buckling; shallow arch; fluid layer

1. Introduction

An arch is termed shallow or flat if the initial height is much smaller than the span. When the lateral load of a shallow arch reaches a critical value the deformed shape may undergo a sudden jump called snap-through. Depending on the lateral load applied; the snap-through buckling of a shallow arch can be divided into two categories: static buckling and dynamic buckling. In the case of static buckling, the lateral load is applied in a quasi-static manner. The first theoretical predication on the static critical load was conducted by Timoshenko (1935), in which a pinned sinusoidal arch was subjected to a uniformly disturbed load. Fung and Kaplan (1952) extended the research by considering a flexibly supported shallow arch under various kinds of lateral loading, including concentrated force acting at the midpoint of the arch. Gjelsvik and Bodner (1962) presented a complete theoretical and experimental analysis on a clamped circular arch under a central concentrated load. Franciosi et al. (1964) extended the conventional limit analysis to the collapse of arches under repeated loading. Roorda (1965) conducted a series of experiments to study the effect of small imperfection on the buckling of elastic structures, including a laterally loaded circular arch. Schreyer and Masur (1966) analysed a clamped circular arch and demonstrated that the existence of a bifurcation of the equilibrium state is not an adequate condition for the use of the asymmetric buckling criterion. Lee and Murphy (1968) considered the inelastic buckling of a clamped circular arch made of work-hardening material. Simitses (1973) studied the effect of an elastic foundation on the critical loads of a sinusoidal arch under disturbed loads.

In the case when the lateral load is applied dynamically instead of in a quasi-static manner, the critical load will be different from the lateral load when it is applied statically. The methodologies used in estimating dynamic critical loads of elastic structures can be classified into two groups. The first approach is to study the total energy and the phase plane of the system. By this method, sufficient conditions for dynamic stability may be established. The first theoretical prediction of dynamic buckling load was conducted by Hoff and Bruce (1954), in which they studied the stability of a sinusoidal arch under unit step loading and ideal impulsive loading. Hsu (1967, 1968) and Hsu et al. (1968) studied the effects of various parameters on the stability of a flexibly supported sinusoidal arch under impulsive and other types of time-varying loads. Xu et al. (2002) considered a shallow arch elastically supported at both ends in the lateral direction and under impulsive loading. Lin and Chen (2003) studied the sufficient condition against dynamic snap-through for a shallow arch under prescribed end motion.

The second approach is to solve the equations of motion numerically to obtain the system response and identify the critical load for specified system parameters. Humphreys (1966) performed both numerical and experimental studies on the dynamic snap-through of a circular arch under uniform impulsive loading. Lock (1966) used both a numerical integration method and an infinitesimal stability analysis to predict the dynamic critical load of a sinusoidal arch under a step loading. Lo and Masur (1976) presented a hybrid method for a snap-through stability analysis, which incorporates an integral equation formulation in conjunction

*Corresponding author. Email: ahmedanwar86@eng.cu.edu.eg

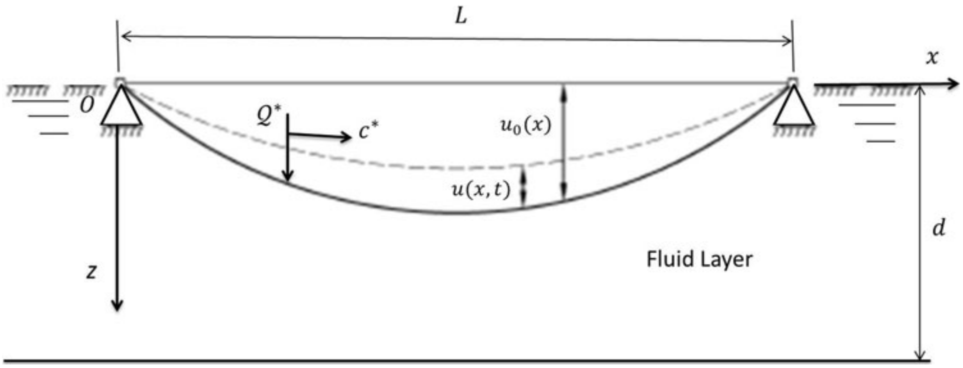

Figure 1. Schematic diagram of a shallow arch resting on a finite fluid layer under a moving point load.

with a finite element method. Johnson (1980) and Johnson and Mclvor (1978) investigated numerically the effects of the spatial distribution of impulsive loads and damping on the dynamic snap-through of a shallow arch. This approach provides a more accurate prediction of the critical load at the expense of a large amount of calculation.

The proposed problem is potentially important because shallow arches have been crucial elements in numerous structures for public transportation. We study this problem to figure out the response and safety of these structures. In this paper, we discuss the effects of finite fluid layer parameters on the stability of a pinned shallow arch under a moving point force (Chen and Lin 2004b; Chen and Li 2006). For instance, Aircraft carriers can be modelled as a shallow arch on a fluid layer.

2. Basic equations

Figure 1 shows an elastic shallow arch with the two pinned-ends being separated by a large distance L. The arch is assumed to be resting on a fluid layer with a finite depth d. The initial shape of the unloaded arch is $z_0(x)$. The arch is subjected to a moving point force Q^* travelling with constant speed c^* from $x = 0$ to $x = L$.

2.1. *Fluid layer equations*

For an incompressible, irrotational, inviscid fluid of constant density ρ_0, the pressure of the fluid $P_f(x, z, t)$ satisfies the following equation, as stated in (Nassar 1987) and El-Refaee (1996),

$$\nabla^2 P_f + \gamma_f P_f = 0. \tag{1}$$

The boundary and initial conditions of the fluid are,

$$\frac{\partial P_f}{\partial z} = \rho_0 \frac{\partial^2 u}{\partial t^2}, \quad \text{at} \quad z = 0 \tag{2}$$

$$\frac{\partial P_f}{\partial z} = 0, \quad \text{at} \quad z = d \tag{3}$$

$$u\,(x, 0) = \frac{\partial u(x, 0)}{\partial t} = 0, \tag{4}$$

where u is the deflection of the arch, $(\gamma_f = \omega/c_f)$ is the fluid wave number, ω is the circular frequency and c_f is the speed of sound in the fluid.

Using the method of separation of variables, we assume the pressure of the fluid as,

$$P_f = u\,(x)\,P\,(z)\,f\,(t). \tag{5}$$

After substituting Equation (5) in Equation (1), we can derive that

$$P\,(z) = ae^{\sqrt{\gamma_f - \lambda^2} z} + be^{-\sqrt{\gamma_f - \lambda^2} z}, \tag{6}$$

where a, b and λ are constants. We can get these constants using the conditions.

Finally, for $f\,(t) = e^{i\omega t}$, we can write the pressure of the fluid as,

$$P_f\,(x, 0, t) = k_f^* u\,(x), \tag{7}$$

where

$$k_f^* = \frac{\rho_0 \omega^2}{\sqrt{\gamma_f - \lambda^2}} \coth\left(\sqrt{\gamma_f - \lambda^2} d\right). \tag{8}$$

2.2. *An arch resting on a fluid layer*

The equation of motion of the arch resting on a fluid layer can be written as stated in Chen and Li (2006),

$$\begin{aligned} \rho_a A u_{,tt} = &-E_a I_a\,(u - u_0)_{,xxxx} + p^* u_{,xx} \\ &-Q^* \delta\,(x - c^* t) - k_f^* (u - u_0), \end{aligned} \tag{9}$$

where k_f^* is the back pressure coefficient of the fluid (indicates the fluid density) as stated in Equation (7). The parameters E_a, ρ_a, A and I_a are Young's modulus, mass density, area and moment of inertia of the cross section of the arch. $\delta(x - c^*t)$ is the Dirac delta function.

In Equation (9), by taking into our account that the span of the arch is long, shear deformation and rotational inertia effects become negligible. We also assume that the effect of the axial stress wave on the lateral vibration is negligible. For a curved beam with slenderness ratio 10, the effect of axial stress wave on the lateral vibration is negligible unless the travelling speed of the point force is in the range of 10 times of the flexural wave speed. In this paper we assume that the moving speed of the point force is well below this range. p^* is the induced axial force which can be considered as independent of the load position x and can be calculated as

$$p^* = \frac{AE_a}{2L} \int_0^L \left(u_{,x}^2 - u_{0,x}^2\right) dx, \tag{10}$$

The boundary conditions of the arch for u at $x = 0$ and L in the general form are

$$u(0) - u_0(0) = u_{,xx}(0) - u_{0,xx}(0) = u(L) - u_0(L) = u_{,xx}(L) - u_{0,xx}(L) = 0. \tag{11}$$

Equations (9) and (10) in non-dimensional forms are

$$w_{,\tau\tau} = -(w - w_0)_{,\xi\xi\xi\xi} + pw_{,\xi\xi} - \frac{\pi}{2}\mathcal{Q}\delta(\xi - c\tau) - k_f(w - w_0), \tag{12}$$

$$p = \frac{1}{2\pi} \int_0^\pi (w_{,\xi}^2 - w_{0,\xi}^2) d\xi, \tag{13}$$

where

$$w = \frac{u}{r}, \quad w_0 = \frac{u_0}{r}, \quad \xi = \frac{\pi x}{L},$$
$$\tau = \frac{\pi^2 t}{L^2}\sqrt{\frac{E_a I_a}{A\rho_a}}, \vdots c = \frac{c^* L}{\pi}\sqrt{\frac{A\rho_a}{E_a I_a}},$$
$$p = \frac{p^* L^2}{\pi^2 E_a I_a}, \quad \mathcal{Q} = \frac{2\mathcal{Q}^* L^3}{\pi^5 E_a I_a r}, \quad k_f = \frac{k_f^* L^4}{E_a I_a \pi^4}, \tag{14}$$

r is the radius of gyration of the cross section. The positive $\mathcal{Q}$ is when the concentrated load points upward in Figure 1, according to Chen and Li (2006). The unstressed shape of the arch before the lateral load is assumed to be in the form

$$w_0(\xi) = h\sin(\xi), \tag{15}$$

h is the rise parameter of the arch (the radius of curvature of the arch).

The shape of the loaded arch is expressed in the Fourier series as

$$w(\xi, \tau) = \lim_{N\to\infty} \sum_{n=1}^{N} \alpha_n(\tau)\sin(n\xi). \tag{16}$$

After substituting Equations (15) and (16) into (12) and (13) we obtain the equations governing α_n,

$$\ddot{\alpha}_n = -n^4\alpha_n - n^2 p\alpha_n - q_n - k_f\alpha_n, \quad n = 1, 2, 3, \ldots. \tag{17}$$

where

$$p = \frac{1}{4}\sum_{m=1}^{\infty} m^2\alpha_m^2 - \frac{h^2}{4}, \tag{18}$$

$$q_1 = \mathcal{Q}\sin(e) - h - k_f h, \tag{19}$$

$$q_n = \mathcal{Q}\sin(ne), \quad n = 2, 3, \ldots \tag{20}$$

$$e(\tau) = c\tau, \tag{21}$$

The parameter $0 < e(\tau) < \pi$ represents the position of the point load on the arch. The overhead dot in Equation (17) represents differentiation with respect to non-dimensional time τ. The initial conditions for Equation (17) are

$$\alpha_1(0) = h, \quad \alpha_n(0) = 0 \quad \text{for} \quad n = 2, 3, \ldots;$$
$$\dot{\alpha}_n(0) = 0 \quad \text{for} \quad n = 1, 2, 3, \ldots \tag{22}$$

3. Snap-through stability

In this section, we study the effects of back pressure of the fluid on the snap-through buckling of a shallow arch when the point load is downward. In the case when a negative point load moves onto the arch quasi-statically, it is clear that the arch will not snap because the net forces prevent the arch from snapping. On the other hand, when the point load moves dynamically with a significant speed, it is not clear whether dynamic snap-through can occur in this case or not. The response history can be calculated by integrating Equation (17) numerically with the initial conditions (22). We analyse the effects of the back pressure of the fluid on the response of the arch with different speeds, where the back pressure of that fluid is a function of some parameters as noted in Equation (8). As stated in Chen and Li (2006), we used only the first four equations in Equation (17) and add damping terms $\mu\alpha_j$ in the equations of motion. It is noted that there is no technical difficulty in using more than four modes in expansion (16) except that the calculation time will increase, where we used until eight modes in expansion (16) and it did not lead to different conclusions. It is obvious in Equation (8) that the back pressure coefficient of the fluid

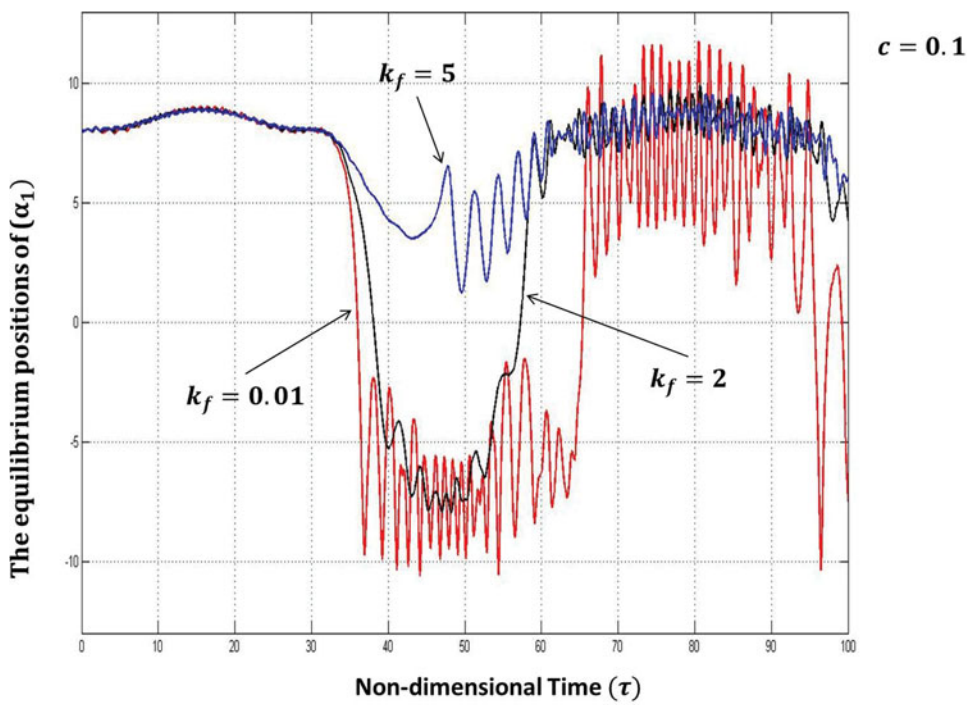

Figure 2. The dynamic response for an arch with $h = 8$, $\mathcal{Q} = -40$ and $c = 0.1$ for different fluids.

is directly proportional to the density of the fluid ρ_0 and the depth of the fluid layer d.

Figure 2 shows the dynamic response of the arch with $h = 8$, $\mathcal{Q} = -40$ and resting on different fluids and the point load moves with $c = 0.1$. The damping parameter μ is chosen to be 0.001 (Chen and Lin 2004b). It is also noted when the point load is downward and moving with small speed, it is obvious the arch will not snap before the load

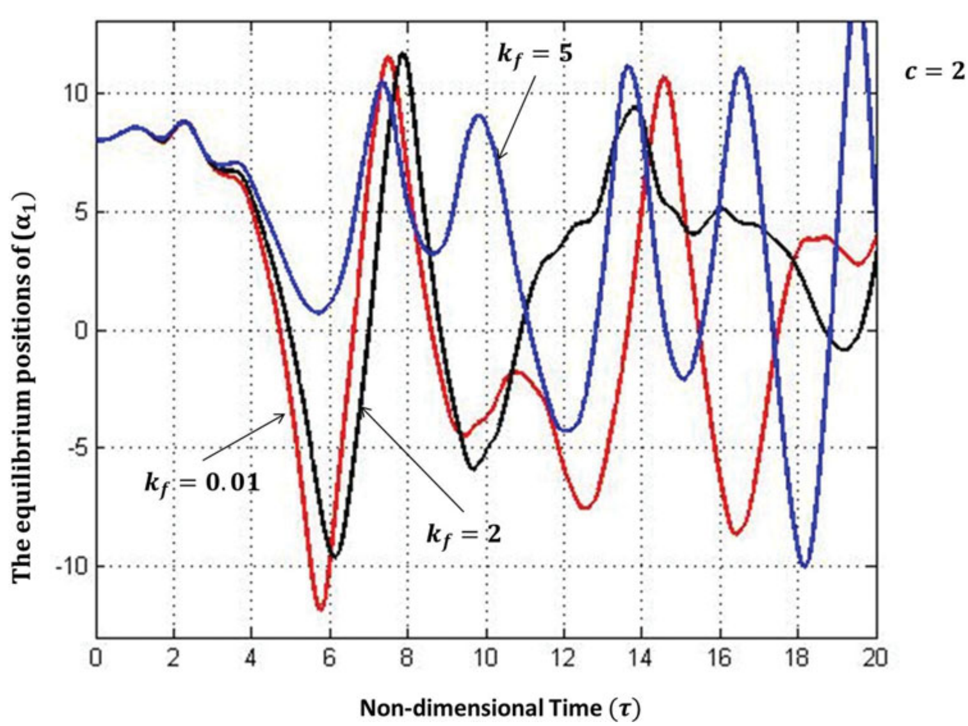

Figure 3. The dynamic response for an arch resting on different fluids with $h = 8$, $\mathcal{Q} = -40$ and $c = 2$.

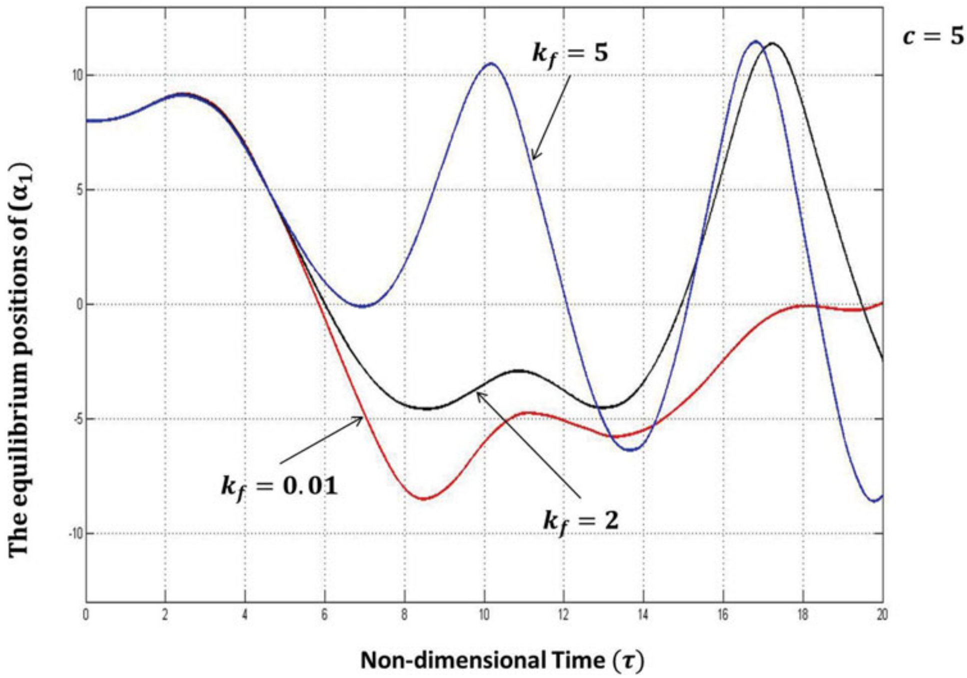

Figure 4. The dynamic response for an arch resting on different fluids with $h = 8$, $Q = -40$ and $c = 5$.

reaches the other end of the arch. It is noted that the arch does not have sufficient time to snap before the load reaches the other end of the arch. Therefore, to determine whether the arch will snap or not after the point load leaves the arch, we have to continue the numerical simulation until the arch settles to one of the stable equilibrium positions, (see, Jones 2003). When the back pressure of the fluid is very small say, $k_f = 0.01$, the arch will snap at $\tau = 36$. For a fluid with further back pressure $k_f = 2$, it is noted that the effects of back pressure is not obvious, where the arch will snap at $\tau = 38$. When $k_f = 5$, the back pressure of the fluid becomes so effective whereas in this case, it is noted that the arch will not snap. There exists a dynamic critical load which is denoted by Q^d_{cr} and depends on the back pressure of the fluid and the speed of the point load. In other words, for a certain fluid the arch will not snap as long as the point load Q is smaller than Q^d_{cr} no matter what the moving speed is. For high speeds, Figure 3 shows an arch resting on different fluids with $h = 8$, $Q = -40$ and $c = 2$. The black dot signifies the instant when the point load leaves the arch. The arch will continue to vibrate after the point load leaves the arch, the calculated results show that the point load leaves the arch at time $\tau = 1.57$. It is noted that the effects of the back pressure of the fluid on the arch, where the arch will snap at $\tau = 4.8$, when $k_f = 0.01$. On the other hand, when $k_f = 2$, the arch will snap at $\tau = 5$. It is concluded that the back pressure of the fluid is not so effective when $k_f < 4.5$. In this case, when the back pressure of the fluid reaches 5, it will be very effective in preventing the arch from snapping, then the arch will begin to snap at $\tau = 11$. Figure 4 shows the calculated α_1 of the arch with $h = 8$, $Q = -40$ for different fluids and very high speed $c = 5$. The point load leaves the other end of the arch at $\tau = 0.63$. It is clear that when the point load moves with very high speed, the arch will be more stable for small back pressure, where the amplitude and ripples of the dynamic response will be directly proportional to the magnitude of the back pressure of the fluid. When the point load leaves the arch, the arch will not oscillate it will snap and then settles to an equilibrium position again.

4. Conclusions

In this paper, we discuss the effects of the back pressure of a fluid layer on the dynamic snap-through of a negative shallow arch under a point load Q moving with a constant speed. It is noted that the back pressure of the fluid is directly proportional to the density of the fluid and depth of the fluid layer. We are interested in studying the stability of the arch, when the load points downward on the arch. It is so obvious that the arch will not snap when the point load moves quasi-statically. On the other hand, when the point load moves with a significant speed, it is noted that the back pressure of the fluid is not so effective on the dynamic snap-through for $k_f < 4.5$. When the point load moves with a very high speed on the arch and rests on a fluid with small back pressure, we notice that the arch is more stable and the amplitude and ripples of the dynamic response of the arch is directly proportional to the back pressure of the fluid. The dynamic critical load depends on the speed of the point load and the back pressure of the fluid.

References

Chen JS, Li YT. 2006. Effects of elastic foundation on the snap-through buckling of a shallow arch under a moving point load. Int J Solids Struct. 43:4220–4237.

Chen JS, Lin JS. 2004b. Dynamic snap-through of a shallow arch under a moving point load. ASME J Vib Acoust. 126:514–519.

El-Refaee MM, Nassar M. 1996. General solution for plastic circular plates resting on a fluid. Int Shipbuilding Prog. 43:119–138.

Franciosi V, Augusti G, Sparacio R. 1964. Collapse of arches under repeated loading. ASCE J Struct Div. 90:165–201.

Fung YC, Kaplan A. 1952. Buckling of low arches or curved beams of small curvature. NACA Tech Note. 2840.

Gjelsvik A, Bodner SR. 1962. The energy criterion and snap buckling of arches. ASCE J Eng Mech Div. 88:87–134.

Hoff NJ, Bruce VG. 1954. Dynamic analysis of the buckling of laterally loaded flat arches. J Math Phys. 32:276–288.

Hsu CS. 1967. The effects of various parameters on the dynamic stability of a shallow arch. ASME J Appl Mech. 34:349–358.

Hsu CS. 1968. Stability of shallow arches against snap-through under timewise step loads. ASME J Appl Mech. 35:31–39.

Hsu CS, Kuo CT, Lee SS. 1968. On the final states of shallow arches on elastic foundation subjected to dynamical loads. ASME J Appl Mech. 35:713–723.

Humphreys JS. 1966. On dynamic snap buckling of shallow arches. AIAA J. 4:878–886.

Johnson ER. 1980. The effect of damping on dynamic snap-through. ASME J Appl Mech. 47:601–606.

Johnson ER, Mclvor IK. 1978. The effect of spatial distribution on dynamic snap-through. ASME J Appl Mech. 45:612–618.

Jones N. 2003. Several phenomena in structural impact and structural crashworthiness. Eur J Mech A/Solids. 22:693–707.

Lee HN, Murphy LM. 1968. Inelastic buckling of shallow arches. ASCE J Eng Mech Div. 94:225–239.

Lin JS, Chen JS. 2003. Dynamic snap-through of a laterally loaded arch under prescribed end motion. Int J Solids Struct. 40:4769–4787.

Lock MH. 1966. The snapping of a shallow sinusoidal arch under a step pressure load. AIAA J. 4:1249–1256.

Lo DLC, Masur EF. 1976. Dynamic buckling of shallow arches. ASCE J Eng Mech Div. 102:901–917.

Nassar M. 1987. Viscoelastic plate resting on fluid. Int Shipbuilding Prog. 34:165–169.

Roorda J. 1965. Stability of structures with small imperfections. ASCE J Eng Mech Div. 91:87–106.

Schreyer HL, Masur EF. 1966. Buckling of shallow arches. ASCE J Eng Mech Div. 92:1–19.

Simitses GJ. 1973. Snapping of low pinned arches on an elastic foundation. ASME J Appl Mech. 2:17–20.

Timoshenko SP. 1935. Buckling of flat curved bars and slightly curved plates. ASME J Appl Mech. 2:17–20.

Xu JX, Huang H, Zhang PZ, Zhou JQ. 2002. Dynamic stability of shallow arch with elastic supports-Application in the dynamic stability analysis of inner winding of transformer during short circuit. Int J Non-linear Mech. 37:909–920.